Journal scientific and applied research, vol. 15, 2019
International Journal

Original Contribution ISSN 1314-6289

GALLIUM NITRIDE POWER ELECTRONICS FOR AEROSPACE - MODELLING AND SIMULATION

Pavlin Gramatikov

SPACE RESEARCH AND TECHNOLOGY INSTITUTE –BAS, BULGARIA;
E-mail: pgramatikov@space.bas.bg,

ABSTRACT: *Modelling and simulation of power GaN HEMT transistors and GaN devices are presented. Comparison and parameters for different GaN products are shown.*

KEYWORD: *GALLIUM NITRIDE, GAN-HEMT, HIGH ELECTRON MOBILITY TRANSISTOR, GAN TRANSISTOR, SIMULATION, MODELLING, GAN POWER DEVICES, SWITCHING POWER SUPPLY DESIGN, POWER SUPPLY EFFICIENCY*

1. Introduction: GaN power devices and drivers

Gallium nitride **(**GaN) is a chemical compound of gallium and nitrogen. GaN has a high critical electric field and high electron mobility. It is the most promising candidates for new high-power, high frequency and high temperature applications. Low and high voltage GaN transistors and diodes based on lateral and vertical structures are considered the future of power electronics [1].

Tables 1, 2, 3, 4, show GaN transistors, and suitable for them driver integral circuits, and their manufactures. GaN applications are: high-energy laser, all-electric planes, unmanned aerial vehicles, robotic vehicles and other [2].

Table 1 GaN transistors

Part Number	Description	Manufacturer
TPH3207WS TP65H050WS-ND TPH3212PS-ND	GANFET N-CH 650V 50A TO247 GANFET N-CH 650V 34A TO247-3 GANFET N-CH 650V 27A TO220	Transphorm
IGOT60R070D1AUMA1 IGLD60R070D1AUMA1DKR	IC GAN FET 600V 60A, Normally OFF, 70 mR IC GAN FET 600V 60A 8SON	Infineon Technologies
GAN063-650WSAQ	650V TO-247	Nexperia USA Inc.
IGT60R190D1SATMA1 IGT60R070D1ATMA1	IC GAN FET 600V 23A 8HSOF MOSFET 600V 23A 55mR CoolGaN	Infineon Technologies
EPC2034	GANFET TRANS 200V 48A BUMPED DIE	EPC
NTP8G202NG	MOSFET N-CH 600V 9A TO220	ON Semiconductor
GS61004B-E01-MR GS-065-011-1-L GS66508B-E01-MR GS61008T	MOSFET 100V 45A E-Mode GaN MOSFET 650V, 11 A, E-Mode GaN MOSFET 650V 30A E-Mode GaN GaN 100V 90A 7mR 100 MHz, 0 V to 6 V	GaN Systems
PGA26E19BA	MOSFET MOSFET 600VDC 190mohm X-GaN	Panasonic

Table 2 GaN MOSFETs with integrated driver

Part Number	Description	Manufacturer
LMG5200 LMG3410R050	80V, 10A, GaN Half-Bridge Power Stage, Up to 10 MHz, 8 pins 480-600, 12A, 50mΩ GaN, int. Driver, current and temp. protection	Texas Instruments
IR11688	200 V Second said Dual Synchronous Rectification Control IC, 8 pins	Infineon Techn.
INN3270C INN3670C	PowiGaN™ technology, 100 W without heat sinks, Constant Power PowiGaN™ technology, 100 W without heat sinks, CV/CC accuracy	Power Integration
NV6117	650 V 120 mΩ GaNFast™ power IC, 2 MHz, Vcc=10-30 V	Navitas

Table 3 One and two gate driver ICs for GaN transistors

Part №	Description	Manufacturer
UCC21220 UCC20225 UCC20225 LMG1210 LMG1020 LMG1205 LM5113 UCC27611 ISO7730 ISO7831	Isolated 3000-V_{RMS} dual-channel gate drivers 4/6 A Isolated Dual-Channel Gate Driver with Single Input, 48-V Systems Isolated 5700-VRMS dual-channel gate drivers 4/6 A 200-V, half-bridge driver, 50-MHz, Single, low-side driver, 60-MHz, 5-V Supply Voltage 80-V Drivers for high-side and the low-side: buck; boost and half bridge 90-V, 1.2-A, 5-A, Half Bridge GaN Driver; buck; boost and half bridge Single-channel, 5-V, 4-A to 6-A Low Side GaN Driver, 100-Mbps, Triple channel digital isolators, 5000 Vrms, Vdd= 2.25 - 5.5 V 100-Mbps, 5.7-kVRMS reinforced triple-channel 2/1 digital isolator	Texas Instruments
1EDF5673 1EDS5663	Isolated 1500 V dual-channel gate drivers for GaN Isolated 6000 V dual-channel gate drivers for GaN	Infineon Technologies
NCP4305A NCP4308A NCP51820	Single second synchronous rectification driver MOSFET, 8 pins, V_{ccon}=4.5 V Single second synchronous rectification driver MOSFET, 8 pins, V_{ccon}=4.5 V 650 V, High−Side and Low−Side Gate Drivers,for GaN Totem Pole PFC	On Semicon-ductor
AN34092B	Single-channel gate driver GaN, (– 5.5V to – 3V), 4.75 V to 24 V Supply	Panasonic
ADuM4120 ADuM4121	Single-channel Gate Driver, Input 2.5-6.6V, Output 2.3A/4.5-35V, 5 kV rms Single-channel Miller clamp, Input 2.5-6.6V, Out 2.3A/4.5-35V, 5 kV rms	Analog Device

Table 4 Control ICs for GaN and MOSFET devices

Part Number	Description	Manufacturer
LM5140-Q1 TPS40400 TPS53632G	Wide Input Range Dual Synchron. Buck Controller, 440 kHz - 2.2 MHz 3 V-20 V, 30 A, PMBus Synchron. Buck Controller, 200 kHz - 2 MHz Half-Bridge Controller ,48-V GaN DC/DC Converter, 300 kHz - 1 MHz	Texas Instruments
IR11688	Half-bridge Synchronous Rectifier Control drives a pair of N-channel	Infineon Techn.
LTC7800 LT1248 LT3798 LT3825 LT8315 LTC1922-1 LTC3765	60 V, High Frequency Step-Down Controller, 320 kHz - 2.25 MHz Power Factor Controller, 500 kHz, Vout=12-17,5V; ON-OFF=12-17,5V Isolated No Opto-Coupler Flyback Controller with Active PFC, CV/CC Isolated No-Opto Synchronous In-Out, Flyback Controller, 250kHz, 18V to 560V/ 630V/300mA Power Switch, CV/CC, Vout=12V Synchronous Phase Modulated Full-Bridge Controller, 1MHz, 6 outputs Active Clamp Forward Isolated Controller and Gate Driver, 430 kHz	Analog Devices
NCP1568	Active Clamp Flyback (ACF) in ZVS, Frequency-100 kHz to 1 MHz	On Semicond.
IRS25411	600 V, 500 KHz buck control ICs for constant LED current regulation.	Int. Rectifier

The AlGaN/GaN heterostructure is now the most used for GaN devices with aerospace applications: for communication and strategic satellites; high altitude aircraft; low earth orbit aircraft; onboard satellites; data communication and networking; especially for high orbits around the Earth; interplanetary flights and work in open space [2]. Some GaN radiation-resistant electronic devices are shown in Table 5. For example, Dual Low-Side Power Driver Module FBS-GAM04-P-R50 is Rad-Hard/Commercially Screened [3]: Guaranteed Total Ionizing Dose – rated to 100 VDS up to 100 % of rated Breakdown and Neutron Fluence – Maintains kRad; Single Event – SEE immunity for LET(Si) of ~83.7 $MeV/mg/cm^2$ with specification up to 1 x 1013 N/cm^2. Suitable Radiation Hardened Low Side GaN FET Drivers are ISL70040SEH and ISL73040SEH.

Table 5 GaN Rad-Hard, Freebird Semiconductor

Part Number	Description
FBS-GAM01-P-R50	50V, 12A Single Low-Side Power Driver Module, 3 MHz, eGaN® FDA10N30X
FBS-GAM01-P-R100	100V, 12A Single Low-Side Power Driver Module, 3 MHz,
FBS-GAM01-P-R-PSE	Single Output eGaN Gate Driver Module
FBS-GAM02-P-R50	50V, 10A Half-Bridge Driver/Logic/integrated output Power GaN HEMTs, 1 MHz,
FBS-GAM02P-R-PSE	50V, High-Speed Multifunctional Power eGaN HEMT Driver
FBS-GAM04-P-R50	50V/10A Dual Low-Side Power Driver Module
FBS-GAM04P-R-PSE	Dual low-side Driver/Logic for use with external power GaN HEMTs
FBS-GAM04-P-R100	100V/10A Dual Low-Side Power Driver Module

Other major providers of GaN parts are: Transphorm; VisIC Tech; Exagan; Sanken Electric; Dialogue Semiconductor; MicroGaN; Toshiba; Oorvo; Macom; Microsemi; NXP Semiconductor; Sumitomo Electric and United Monolithic [2, 4, 5, 6, 7, 8]. Figure 1 shows comparison and advantages of different structures of GaN transistors, according to the specification of different manufacturers [9].

Drivers suitable for HEMT GaN are ADuM4120 and ADuM4121 – isolated, single-channel drivers that employ Analog Devices, Inc. iCoupler® technology to provide precision isolation – 5 kV rms isolation.

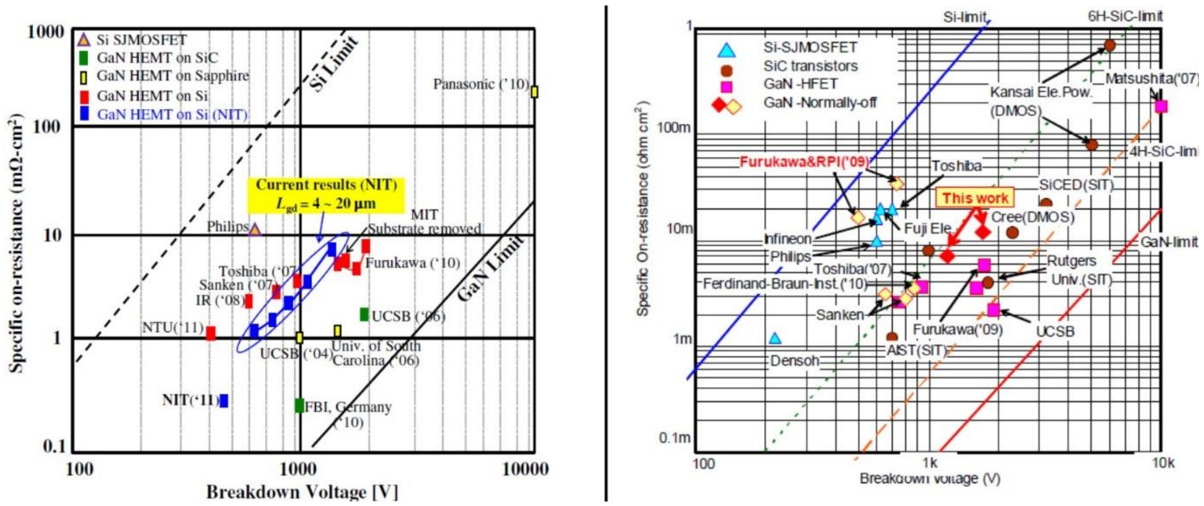

Fig. 1 Comparison and benchmark for different GaN manufactures [9].

Application examples for GaN device are: Power Factor Correction (PFC) totem pole circuit with efficiency of 99 %; Active clamp Flyback with size reduction of 60 % and Motor drive 3 phase Inverter circuit (size reduction of 75 % and loss reduction of 60 %).

2. Modelling and topologies for power electronics

The aim of this work is to study main working stages and different parameters of bidirectional isolated PFC dual active bridge (PFC-DAB) AC–DC converter topology. A bidirectional and isolated (DAB) AC–DC converter topology with power destiny =1,34 W/cm^3 is given on Figure 2 [10,11]. One article [12] discusses the advantages when high-performance vertical GaN transistors and diodes are used in the DAB AC–DC converter. Totem pole topology PFC advantages are shown in Figure 3 [13]. Reference [14] explains how hard-switching can form a fundamental switching transition for GaN devices.

For $S_{SR,1}$ and $S_{SR,2}$ and his drivers (Figure 2, GaN half-bridge topology) it is suitable plate LMG341xEVM-018 [15].

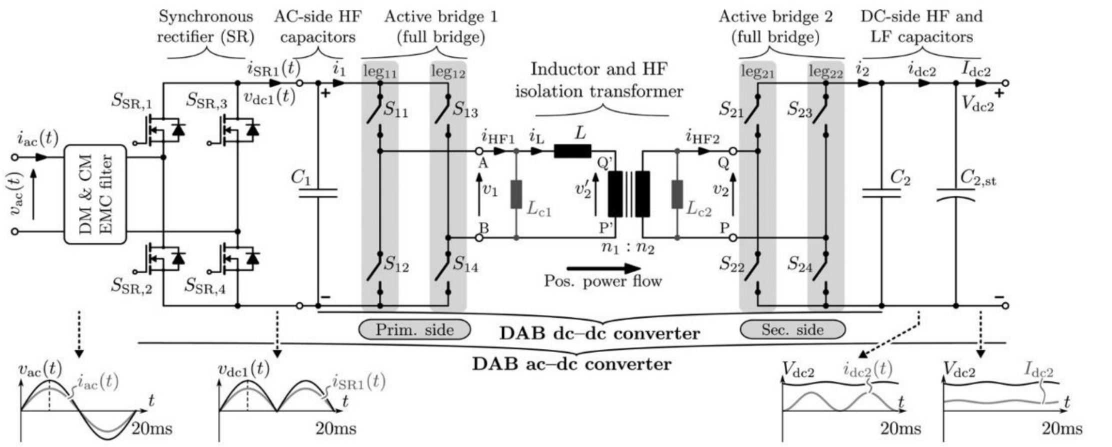

Fig. 2 Circuit schematic of the single-phase, single-stage (1-S), bidirectional and isolated DAB AC–DC converter topology [10].

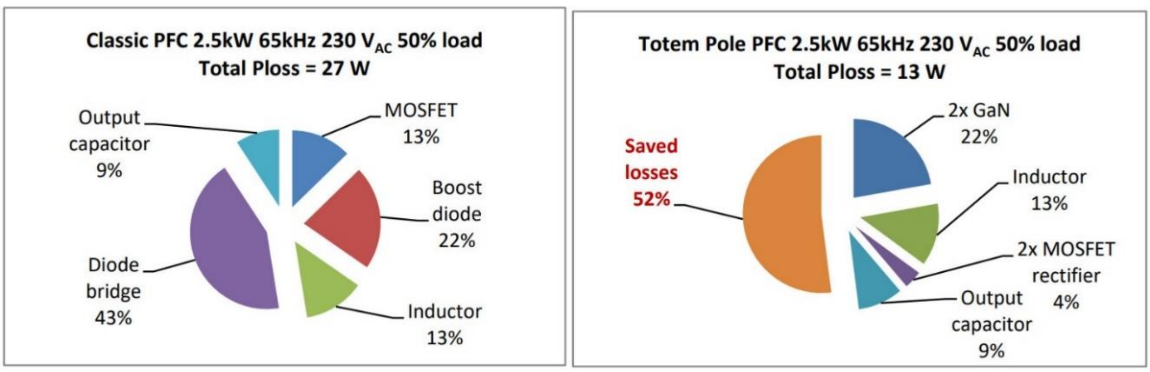

Fig. 3 Comparison between classic boost PFC vs. totem pole PFC [13].

3. Simulation and results of GaN topology with aerospace application

Figure 4 shows work of the Motor1 from source V2. The design parameters for Figure 4 are: V_2=44-132 Vac; $V_{2\text{-nom}}$=110 Vac; F_{ac}=50 Hz (to $V_{2\text{-min}}$=44 Vac); F_{ac}=150 Hz (to $V_{2\text{-max}}$=132 Vac); V_{C1}=193 Vdc; V_{C2}=8,4 Vdc; F_{sw}=50-400 KHz and P_{out}=1250 W. We can calculate L1, when $V_{ac\text{-nom}}$ is applied:

$$L_1 = \frac{1}{\%Riple}\frac{V2\_nom^2 * (1-1{,}41\frac{V2\_nom}{Vc1})}{Fsw * Pout} = \frac{1}{25\%}\frac{110^2 *(1-1{,}41\frac{110}{193})}{75 * 10^3 * 1250} = 101\ uH \tag{1}$$

Maximum RMS current occurs in L1 when Vac = 44 V:

$$I_{L1\_rms}\frac{Pout}{\eta * V2\_min} = \frac{1250}{0{,}95 * 44} = 29{,}9\ Arms \tag{2}$$

Voltage ripple peak to peak (Vac_pp) of V_{C1}, when Vac = 44 V:

$$V_{ac\_pp} = \frac{Pout}{2\pi *\ Fsw * Vc1 * C1} = \frac{1250}{2*3{,}14*75*10^3*193*0{,}47*10^{-3}} = 29\ V \tag{3}$$

The PFC output capacitor capacitance, when Vac = 44 V:

$$C_1 = \frac{Pout}{2\pi * Vc1 * Fsw * Vac\_pp} = \frac{1250}{2*3{,}14*193*75*10^3*29} = 474\ uF \tag{4}$$

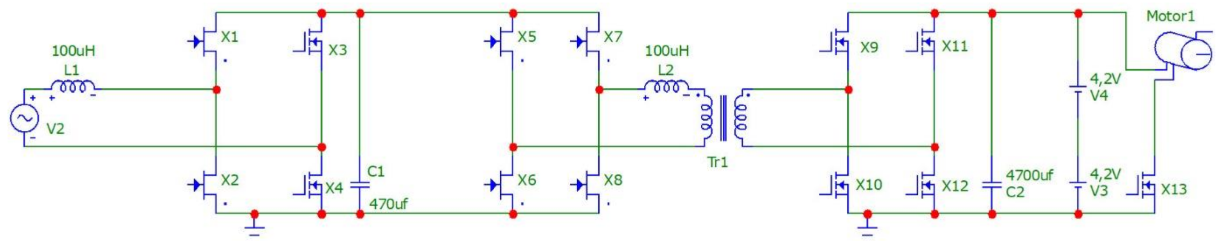

Fig. 4 Single-phase generator to: PFC; DC–DC converter; battery and motor.

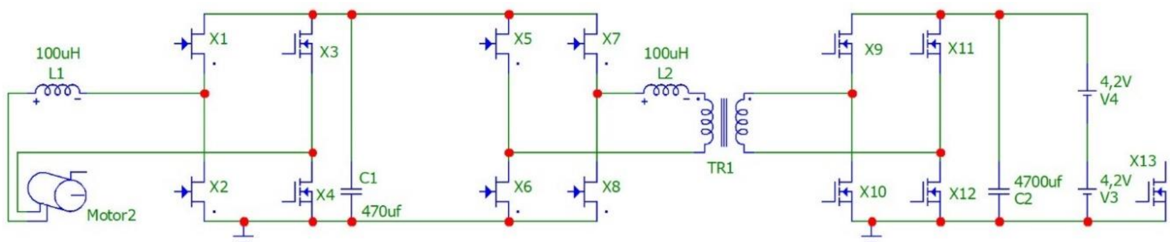

Fig. 5 Battery to: isolated DC–DC, PFC-full bridge converter, and motor.

For Figure 4 and Figure 5 (made with Micro-Cap 12.2.0.3 soft) the following transistors were chosen: for X1,2–GS66516B (650 V/ 60 A/ 25 mΩ); for X3,4–IXFK210N30X3 (300 V/ 210 A/ 5,5 mΩ/ 1250 W); for X5,6,7,8–X2LMG3411R050 (480 V/ 12 A/ 50 mΩ/ $V_{DD(ON)}$=9,1 V/ 27 mA/ 500 Khz) and IPT004N03LATMA1 (30 V/ 300 A/ 0,40 mΩ/ 300 w) for X9,10,11,12,13.

GaN device X2LMG3411R050 inside the case has a driver with over-temperature protection (when temperature exceeds 165 °C) and cycle-by-cycle overcurrent protection (40-77 A). This driver works together with triple channel digital isolators ISO7730/1 [15].

Simulation PFC start up from Figure 4 (when Vac = 132/44 Vac and time interval of 1-3 s) shown at Figure 6 for L1, X1-4, C1 (made with PLECS soft).

In vertical order are shown; input voltage V_2; current I_{L1} and voltage V_{C1}. Zoom view of the transition mode is shown on Figure 7 for: V_2; I_{L1}; input voltage of X2 and $V_{C1.}$ Figure 8 shows a zoom of the established mode for: V_2; I_{L1} and V_{C1}. Tables 6,7,8,9 (made with PLECS) give simulation values for Figure 4 for X1-4 (four transistors GS66516B per switch X1,2 and two IRFP4668PBF for X3,4), when L1 is optimal changed versus $F_{sw;}$ and P_{out}=1250 W.

Table 6 shows negative result at V_2=44 Vac/50 Hz where the temperature losses of X1,2,3,4 are unacceptably high; at Fsw =400 KHz, 3 seconds after switching on, the transistors X1,2 overheat and their thermal protection is activated. Table 7 shows positive results at V_2=55 Vac: the temperature losses of X1-4 are acceptable; the temperature protection does not trip and efficiency of X1-4 rises above the desired minimum 90 %, for Fsw=50-75 [KHz]. Table 8,9 shows excellent results at V_2=110-132 Vac: the temperature losses are sufficiently low and with Effiency=95,96-97,66 % it is possible to work with more than 75 KHz, which reduces the weight of the radiators and L1 up to 4 times.

Table 6 Parameters of L1, X1-4 from Figure 4, when V_2=44 Vac/50 Hz.

F_{sw} [KHz]	50	75	100	200	300	400
X1,2,3,4 losses [W]	236,15	243,95	251,06	279,65	306	Over / 3 s
L2 [uH]	470	313	235	117	78	59
Effiency [%]	81,14	80,51	79,96	77,76	75,56	X

Table 7 Parameters of L1, X1-4 from Figure 4, when V_2=55 Vac/62,5 Hz

F_{sw} [KHz]	50	75	100	200	300	400
X1,2 Losses [W]	14,04	16,76	19,47	30,64	41,63	53,8
X3,4 Losses [W]	104,9	106.7	108,53	116,9	122,59	132
L2 [uH]	470	313	235	117	78	59
Effiency [%]	90,49	90,13	89,77	88,28	86,87	85,24

Table 8 Parameters of L1, X1-4 from Figure 4, when V2=110 Vac/125 Hz.

F_{sw} [KHz]	50	75	100	200	300	400
X1,2 Losses [W]	3,77	5,28	6,80	12,86	19,36	25,13
X3,4 Losses [W]	21,82	22,12	22,23	23,84	24,38	25,23
L2 [uH]	470	313	235	117	78	59
Effiency [%]	97,93	97,80	97,66	97,09	96,50	95,96

Table 9 Parameters of L1, X1-4 from Figure 4, when V2=132 Vac/150 Hz

F_{sw} [KHz]	50	75	100	200	300	400
X1,2 Losses [W]	3,16	4,55	5,93	11,46	17,35	21,76
X3,4 Losses [W]	15,13	15,26	15,43	16,07	16,80	17,18
L2 [uH]	470	313	235	117	78	59
Effiency [%]	98,52	98,40	98,28	97,78	97,27	96,87

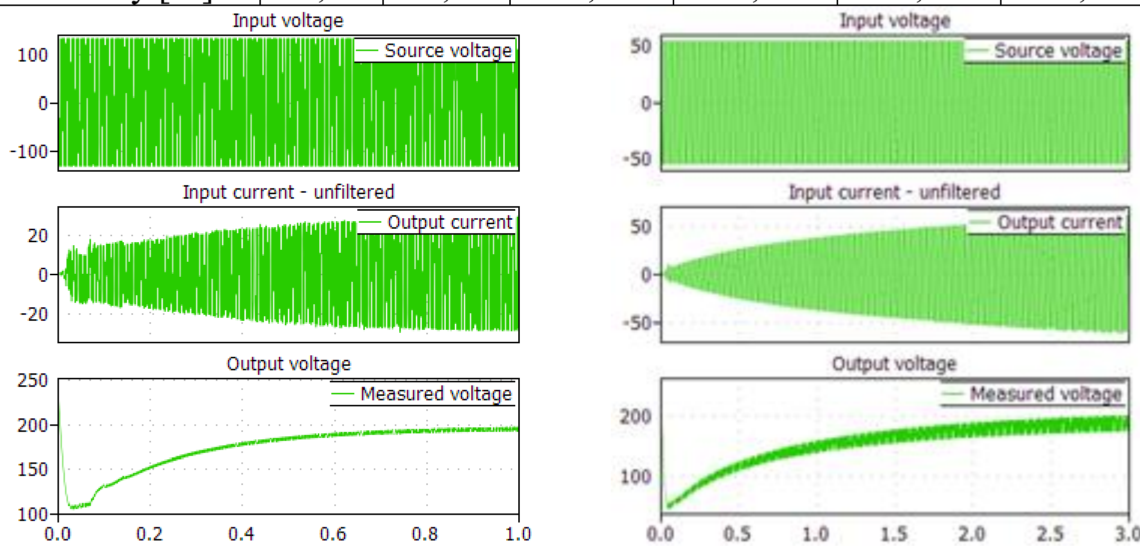

Fig. 6 Start process of Fig. 4 at V_2 = 132/55 Vac.

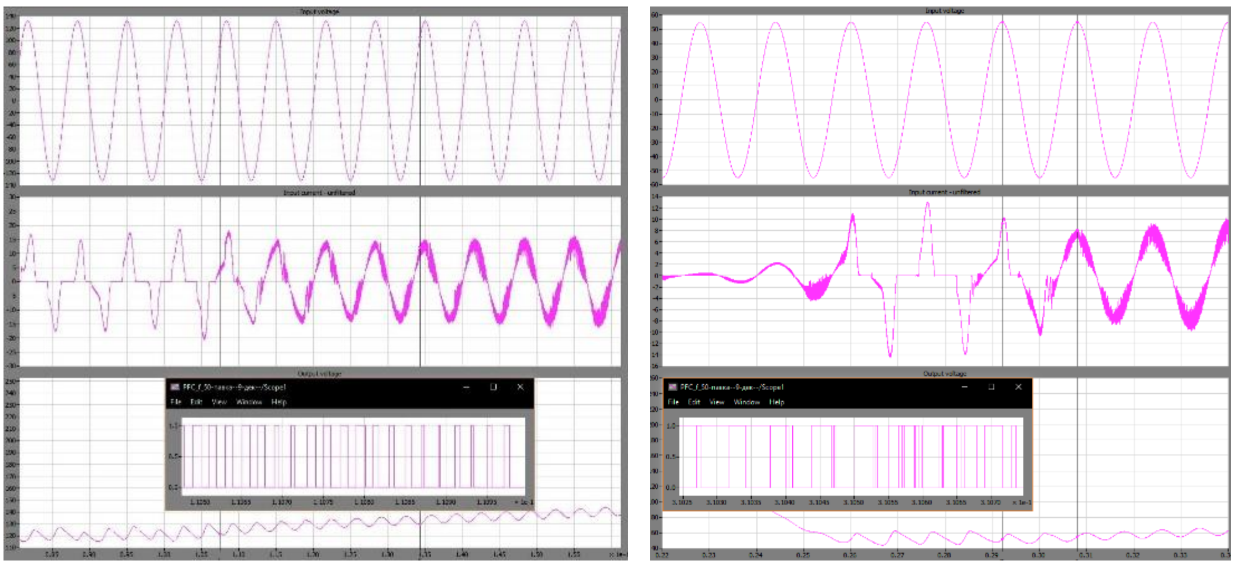
Fig. 7 Processes of Fig. 4 – zoom of transition mode when V_2 = 132/55 Vac.

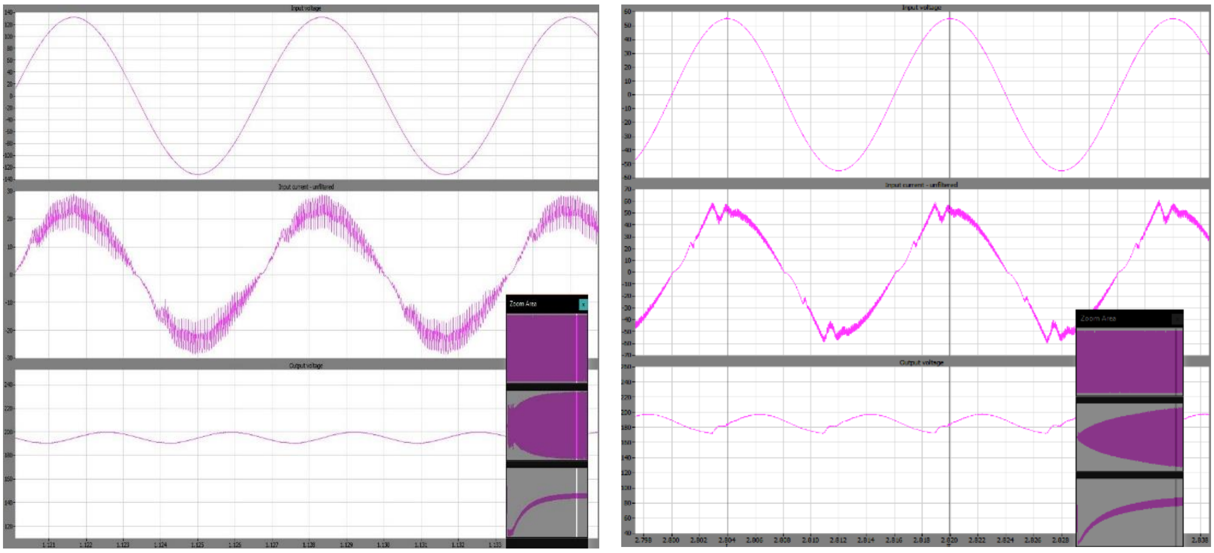

Fig. 8 Processes of Fig. 4 – zoom of established mode when V_2 = 132/55 Vac.

Table 10 Parameters from Figure 4 for L2, X5-8 versus F_{sw}.

F_{sw2} [KHz]	50	100	200	300	400	500
X5,6,7,8 Losses [W]	2,15	2,99	4,46	5,62	19,7	23,66
L2 [uH]	16,9	8,4	4,2	2,8	2,1	1,7
Effiency [%]	99,83	99,59	99,65	99,56	98,42	98,02

For Figure 4 simulation gives for first full bridge circuit the following results (for X5,6,7,8 and when F_{sw} =75 KHz): switching loss P_{sw}=0,23 W; conduction loss P_{on}=2,61 W; junction temperature 27 °C; L2=11,2 uH; efficiency 99,8 %. To reduce the weight of L2, Tr1 and radiators of X5,6,7,8, simulations were made at F_{sw2}=50-400 KHz, see Table 10. In second full bridge circuit for one transistor X9 (or X10,11,12) the dependencies (5,6,7,8,9) are in effect, where: P_{on} is power loss during ON-state; R_{on} is drain-source on-state resistance; P_{sw} is source-drain switching loss; Pg is gate switching loss; Eon_off is the drain switching loss energy (from manufacturer's data); Vg is gate voltage; Qg is total gate charge; Iss is steady state gate current.

$$I_{rms} = \frac{Pout}{Vout}\sqrt{0{,}5} = \frac{1250*0{,}7071}{8{,}4} = 105{,}22\ A_{rms} \tag{5}$$

$$P_{on} = {I_{rms}}^2 * R_{on}(80°C) = 105{,}22^2 * 10^{-3} * 1{,}4 = 15{,}5\ W \tag{6}$$

$$P_{sw} = E_{on-off} * Fsw2 = 6{,}4 * 10^{-3} * 300 * 10^3 = 1{,}92\ W \tag{7}$$

$$P_g = Vg * Qg * Fsw2 = 9 * 336 * 10^{-9} * 300 * 10^3 = 0{,}9072 W \tag{8}$$

$$P_{tot} = P_{on} + P_{sw} + P_g = 15{,}5 + 1{,}92 + 0{,}91 = 18{,}33\ W \quad (9)$$

For Figure 4 four transistors X9,10,11,12 will dissipate 18,33*4=73,32 W, or $Effiency_{9,10,11,12}$=100*(1250-73,52)/1250=94,13 %. With work parameters for Figure 4: V2 = 110 V; F_{sw} = 200 KHz; F_{sw2} = 300 KHz. Total in Figure 4 (for transistors X1-12) $Effiency_{1\text{-}12}$ = 100*0,9709 * 0,9956 * 0,9413 = 90,99 %.

3. Conclusion

When we want to reduce the weight of hybrid electric propulsion system, we must reduce the need for heat dissipation by improving energy efficiency [16]. Bidirectional, dual active bridge is suitable for level 3 electric vehicle charging stations [17]. GaN MOSFETs are suitable for Unmanned Aerial Vehicles BLDC Motor Drive [18].

This work exposes original modelling and simulation development of a primary power supply. Parameters for GaN transistors and circuit solution are chosen and verified by simulations. The author has a serial works for primary power supplies; power supply efficiency; GaN power devices, switching power supply design, power supply efficiency [19,20].

Reference:

[1]. Jie Hu, Yuhao Zhang, Min Sun, Daniel Piedra, Nadim Chowdhury, Tomás Palacios, Materials and processing issues in vertical GaN power electronics, Elsevier Materials Science in Semiconductor Processing, Volume 78, May 2018, pp. 75-84. https://doi.org/10.17660/ActaHortic.2016.1134.29

[2]. Body of Knowledge (BOK): Gallium Nitride (GaN) Power Electronics for Space Applications, NEPP Electronics Technology Workshop (ETW), NASA GSFC, Greenbelt, MD, June 17-20, 2019, 22 p. https://ntrs.nasa.gov/archive/nasa/casi.ntrs.nasa.gov/20190033097.pdf

[3]. Freebird Semiconductor High Reliability GaN HEMT discrete devices. https://www.freebirdsemi.com/universal-gams/

[4]. Ultra High Speed Driver for GaN FET, uP1964, uP1966A, uP1966D. https://upisemi.com/gan/

[5]. Product Selector Guide for eGaN FETs and ICs, 2019, 5 p. https://epc-co.com/epc/Portals/0/epc/documents/guides/EPCeGaNFET_selector_guide.pdf

[6]. X-GaN by Panasonic has adopted the HD-GIT structure. https://industrial.panasonic.com/kr/products/semiconductors/powerics/ganpower

[7]. High-speed FET Driver, 40 MHz: PE29100; PE29101; PE29102. https://www.psemi.com/products/gan-fet-driver

[8]. Mansilla O. E., J. Broline, H. Satterfied, L. G. Pearce, E. J. Thomson, Low side GaN Fet Driver for Space Applications, ESPC 2016, E3S Web of Conferences 16, 12006 (2017), 4 p., DOI: 10.1051/e3sconf/20171612006 https://www.e3s-conferences.org/articles/e3sconf/pdf/2017/04/e3sconf_espc2017_12006.pdf
[9]. Sque Stephen, High-voltage GaN-HEMT devices, simulation and modelling, NXP Semiconductors, ESSDERC 2013, Bucharest, Romania 16th September 2013, 73 p. https://www.stevesque.com/publications/Sque-GaN-ESSDERC-2013.pdf
[10]. Everts Jordi, F. Krismer, J. Van den Keybus, J. Driesen, J. W. Kolar, Optimal ZVS Modulation of Single-Phase Single-Stage Bidirectional DAB AC-DC Converters, IEEE Transactions on Power Electronics, Vol. 29, No. 8, pp. 3954-3970, August 2014, pp. 3954-3970. https://ieeexplore.ieee.org/abstract/document/6671445
[11]. Everts Jordi, Modeling and Optimization of Bidirectional Dual Active Bridge AC–DC Converter Topologies, Dissertation for the degree of Doctor in Engineering Science, ARENBERG DOCTORAL SCHOOL, FACULTY OF ENGINEERING SCIENCE, March 2014, 360 p. https://core.ac.uk/download/pdf/34593682.pdf
[12]. Taube Andrzej, Mariusz Sochacki, Jan Szmidt, Eliana Kaminska, Anna Piotrowska, Modelling and Simulation of Normally-Off AlGaN/GaN MOS-HEMTs, INTL Journal of Electronics and Telecomumunications, 2014, VOL. 60, NO. 3, pp. 253–258, revised September, 2014. https://doi.org/10.1016/j.mssp.2017.09.033
[13]. CoolGaN™ totem-pole PFC design guide and power loss modelling.
[14]. https://www.infineon.com/dgdl/Infineon-Design_guide_Gallium_Nitride-CoolGaN_totem-pole_PFC_power_loss_modeling-ApplicationNotes-v01_00-EN.pdf?fileId=5546d4626d82c047016d95daec4a769a
Sandeep R. Bahl, Daniel Ruiz, Dong Seup Lee, Product-level Reliability of GaN Devices Sandeep R. Bahl, Daniel Ruiz and Dong Seup Lee, Texas Instruments, 2900 Semiconductor Dr. Santa Clara, CA 95052, 7 p. https://www.ti.com/lit/ml/slyy093/slyy093.pdf
[15]. Using the LMG341xEVM-018 half-bridge and LMG34XXBB-EVM breakout board EVM, https://www.ti.com/lit/ug/snou165a/snou165a.pdf
[16]. Junghsen Lieh, Eric Spahr, Design of Hybrid Propulsion Systems for Unmanned Aerial Vehicles, 47th AIAA/ASME/SAE/ASEE Joint Propulsion Conference&Exhibit, 31 July - 03 Aug 2011, San Diego, California, 1-14 p. https://pdfs.semanticscholar.org/74ee/71c7e7ae5da70a331e82c6530e1a03cdb420.pdf
[17]. Bi-directional, dual active bridge reference design for level 3 electric vehicle charging stations, 14 Jun 2019, http://www.ti.com/tool/TIDA-010054

[18]. Donato Repole, Leslie R. Adrian, Evaluation of GaN MOSFET for Unmanned Aerial Vehicles BLDC Motor Drive, 2018 IEEE 59th International Scientific Conference on Power and Electrical Engineering of Riga Technical University (RTUCON), 12-13 Nov. 2018, DOI: 10.1109/RTUCON.2018.8659885
[19]. Gramatikov P., P. Getsov, Electronic control of motor-generators for unmanned aerial vehicles, 6 International scientic and technical conference “Engineering, technologies, education, security’’ 30.5-02.06.2018 Veliko Tarnovo, Yssue 2 (5), Sofia, 2018, pp. 122-125, ISSN 2535-0315(Print), ISSN 2535-0323 (Online), https://techtos.net/sbornik/2-2018.pdf
[20]. Gramatikov P., New power electronics technologies with aerospace application, Fifteenth International Scientific Conference "Space, Ecology, Safety", BULGARIAN AC ADEMY OF SCIENCES, Space Research and Technology Institute, 6 – 8 November 2019, Sofia, Bulgaria, pp. 119-125. ISSN 2603 – 3313 (Print), ISSN 2603 – 3321 (Online), http://www.space.bas.bg/SES/archive/SES%202019_DOKLADI/2_Aerospace%20Technologies/8_Gramatikov.pdf